

# Closed loop control of Diode Clamped Multilevel Inverter with Integrated Maximum Power Point Tracking for Grid Connected Photovoltaic Application

**Abstract.** A Three-phase Diode clamped multilevel inverter (DCMLI) based photovoltaic system for grid connection is proposed with different maximum power point tracking (MPPT). This photovoltaic (PV) system utilizes two conversion stages: algorithm for tracking the maximum power point and a DCMLI used as an interfacing unit. The maximum power point tracking is achieved with Perturb and absorb (P&O), Incremental conductance algorithm (INC) and a fuzzy logic controller (FLC), and the DCMLI regulates the DC link voltage and synchronizes the grid voltage and current in order to achieve unity power factor operation. The proposed system provides high dynamic performance in terms of Total Harmonic Distortion (THD) and power quality injected into the grid. The validity of the proposed system is confirmed by simulations.

**Streszczenie.** Opisano trójfazowy przekształtnik wielopoziomowy DCMLI przystosowany do sieci fotowoltaicznej z układem śledzenia maksymalnej mocy MPPT. System wykorzystuje dwa etapy konwersji: algorytm do śledzenia maksymalnej mocy i przekształtnik użyty jako interfejs. Interfejs steruje napięciem DC i synchronizuje napięcie sieci. (Wielopoziomowy przekształtnik ze zintegrowanym układem śledzenia maksymalnej mocy w zastosowaniu do połączeń z siecią fotowoltaiczną)

**Keywords:** Fuzzy Logic Controller, Incremental conductance algorithm, Perturb and absorb, solar MPPT, THD.

**Słowa kluczowe:** sterownik fuzzy-logic, układ śledzenia maksymalnej mocy, sieć fotowoltaiczna, przekształtnik

## 1. Introduction

Renewable energy sources, such as solar, wind, biomass, etc., are desirable for electrical power generate due to their unlimited existence and environmental friendly nature [1]. Global warming and energy policies have become a hot topic on the international agenda in the last years. Developed countries are trying to reduce their greenhouse gas emissions. In this context, photovoltaic (PV) power generation has an important role to play due to the fact that it is a green source. The only emissions associated with PV power generation are those from the production of its components. After their installation they generate electricity from the solar irradiation without emitting greenhouse gases. Because of the photovoltaic nature of solar panels, their current-voltage, or IV, curves depend on temperature and irradiance levels [2]. Therefore, the operating current and voltage which maximize power output will change with environmental conditions, as in Figure 1. There are a number of maximum power point tracking (MPPT) algorithms which track the optimal current and voltage in a changing environment such as the model-based method [3], perturbation & observation (P&O) method [4], [5], incremental conductance method [6] and fuzzy logic method [7]. Multilevel inverters put forward many benefits for higher power applications. In particular, these include ability to synthesis the voltage waveforms with lower harmonic content than 2-level inverters and operation at higher DC voltages using series connected semiconductor switches. While many different multilevel converter topologies have been proposed, the two most common topologies are the Cascaded Inverter and its derivatives [8], [9] and the Diode Clamped inverter [10]. The two most popular switching strategies for these multilevel inverter topologies are Carrier based PWM and Space Vector PWM (SVPWM) [11] modulation.

The proposed system consists of a PV array connected to the three phase five-level Diode clamped inverter through a DC bus (from PV array) which is connected to an ideal grid as shown in Fig. 3 [11]

The control structure of the grid-connected PV system is composed of two structure control.

1. The MPPT control, whose main function is to take out the maximum power from the PV array.
2. The inverter control.

- i. To control the DC bus voltage.
- ii. To ensure high quality of the injected power.

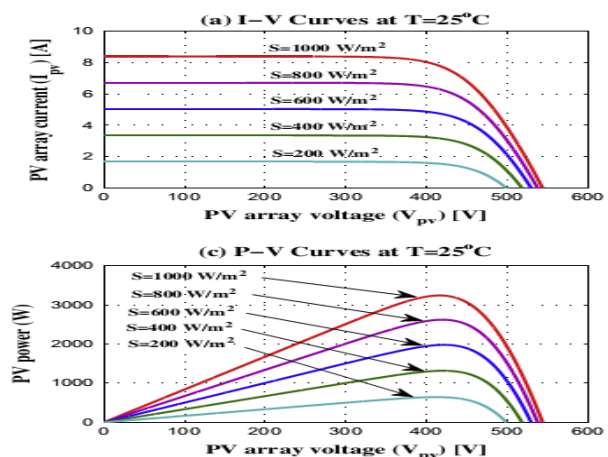


Fig.1. Charecterics of photovoltaic system

## 2. System descriptions

The structure of the entire power circuit is shown in Fig.3 in which the inverter control is discussed in two methods that are SPWM and SVPWM. The circuit consists of PV array, multi level inverter, MPPT controllers which process voltage and current from PV array and generates pulses to IGBT connected across Inverter, PI Controller and the Grid filter and grid. The PV array can produce a maximum power of 3 kW at a solar irradiance of 1 kW/m<sup>2</sup> and ambient temperature of 25°C. The PV array for the proposed system is KC200GT and it is simulated under solar radiation of 1000 W/sq.m and ambient temperature of 25°C using a model based on [13].

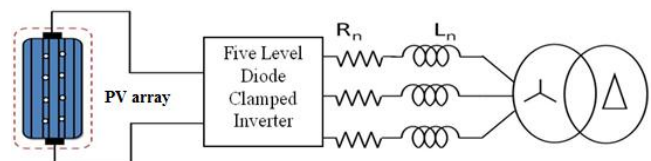


Fig.2. General Diagram of Grid Connected photovoltaic system

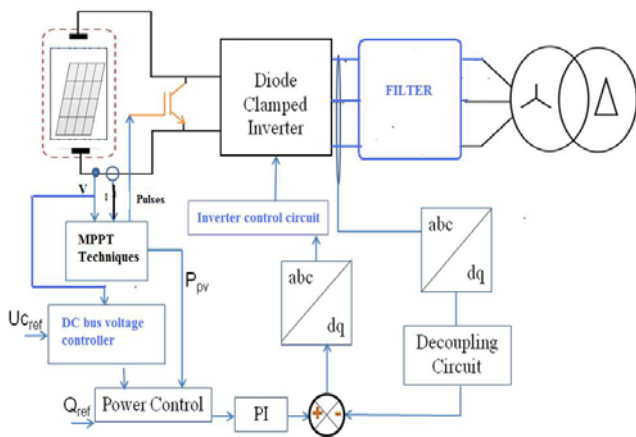


Fig.3. Block diagram for the proposed scheme

### 3. MPPT algorithms

#### 3.1. Perturbation and Observation (P&O) Method

This method [14], [15] is the most commonly used algorithm to track the maximum power due to its simple configuration and less required parameters. This method finds the maximum power point of PV modules by means of iteratively perturbing, observing and comparing the power generated by the PV modules. It is broadly applied to the maximum power point tracker of the photovoltaic system for its features of simplicity and convenience. According to the structure of MPPT system shown in Fig. 3, the required parameters are only the voltage and current of PV array. Fig. 4 shows the relationship between the terminal voltage and output power generated by a PV module. It can be experiential that in spite of the magnitude of sun irradiance and terminal voltage of PV modules, the maximum power point is obtained while the condition  $dp/dv = 0$  is accomplished. The slope  $dp/dv$  of the power can be intended by the successive output voltages and output currents, and can be expressed as follows,

$$(1) \quad \frac{dp(n)}{dv} = \frac{p(n) - p(n-1)}{v(n) - v(n-1)}$$

where  $p(n) = v(n)I(n)$

In Fig. 4, if the operating voltage of the PV array is perturbed in a given direction and  $dP/dV > 0$ , it is known that the perturbation moved the array's operating point toward the MPP. The P&O algorithm would then continue to perturb the PV array voltage in the same direction.

If  $dP/dV < 0$ , then the change in operating point moved the PV array away from the MPP, and the P&O algorithm reverses the direction of the perturbation. This algorithm is summarized in Table 1. The process is periodically repeated until the MPP is reached. The advantage of the P&O method is that it is easy to implement. However, it has some restrictions, like oscillations around the MPP in steady state operation, slow response speed, and even tracking in wrong way under rapidly changing atmospheric conditions.

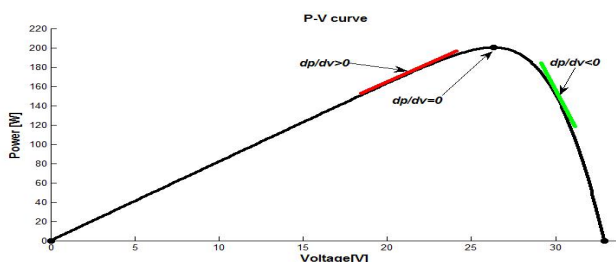


Fig.4. P-V characteristic of a PV module

The system oscillates around the MPP, which causes power loss. The oscillation can be minimized by decreasing the size of the perturbation. However, a too small perturbation slows considerably tracking the MPP. Then there is a compromise between accuracy and speed.

Table 1. Summarized algorithm of P&O

Perturbation	Change in power	Next perturbation
Positive	Positive	Positive
Positive	Negative	Negative
Negative	Positive	Negative
Negative	Negative	Positive

#### 3.2. Incremental Conductance (INC) Method

The theory of the incremental conductance method [14],[15] is to determine the variation direction of the terminal voltage for PV modules by measuring and comparing the incremental conductance and instantaneous conductance of PV modules. If the value of incremental conductance is equal to that of instantaneous conductance, it represents that the maximum power point is found. The basic theory is illustrated with Fig. 5.

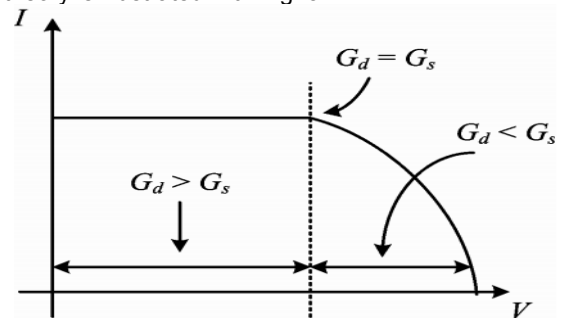


Fig.5. The schematic diagram of the INC method

When the operating behavior of PV modules is within the constant current area, the output power is proportional to the terminal voltage. That means the output power increases linearly with the increasing terminal voltage of PV modules (slope of the power curve is positive,  $dp/dv > 0$ ). When the operating point of PV modules passes through the maximum voltage, its operating behavior is similar to constant voltage. Therefore, the output power decreases linearly with the increasing terminal voltage of PV modules (slope of the power curve is negative,  $dp/dv < 0$ ). When the operating point of PV modules is exactly on the maximum power point, the slope of the power curve is zero  $dp/dv = 0$  and can be further expressed as,

$$(2) \quad \frac{dP}{dV} = \frac{d(VI)}{dV} = I \frac{dP}{dV} + V \frac{dI}{dV} = I + V \frac{dI}{dV}$$

By the relationship of  $dp/dv = 0$

$$(3) \quad \frac{dI}{dV} = -\frac{I}{V}$$

$dI$  and  $dV$  represent the current error and voltage error before and after the increment respectively. The INC can track rapidly increasing and decreasing irradiance conditions with higher correctness than P&O. [16] However, because of noise and errors due to measurement and quantization, this method also can produce oscillations around the MPP; and it also can be confused in rapidly changing atmospheric conditions. One more drawback of this algorithm is the increased complication when compared to perturb and observe. This increases computational time, and slows down the sampling frequency of the array voltage and current [16].

The static conductance ( $G_s$ ) and the dynamic conductance ( $G_d$ , incremental conductance) of PV modules are defined as follows,

$$(4) \quad G_s = -\frac{I}{V}$$

$$(5) \quad G_d = -\frac{dI}{dV}$$

The maximum power point (operating voltage is  $V_m$ ) can be found when

$$(6) \quad G_d = G_s$$

When the equation in (3) comes into existence, the maximum power point is tracked by MPPT system. However, the following situations will happen while the operating point is not on the maximum power point:

$$(7) \quad \frac{dI}{dV} > \frac{I}{V}; \left( G_d > 0, \frac{dP}{dV} > 0 \right)$$

$$(8) \quad \frac{dI}{dV} < -\frac{I}{V}; \left( G_d < G_s, \frac{dP}{dV} < 0 \right)$$

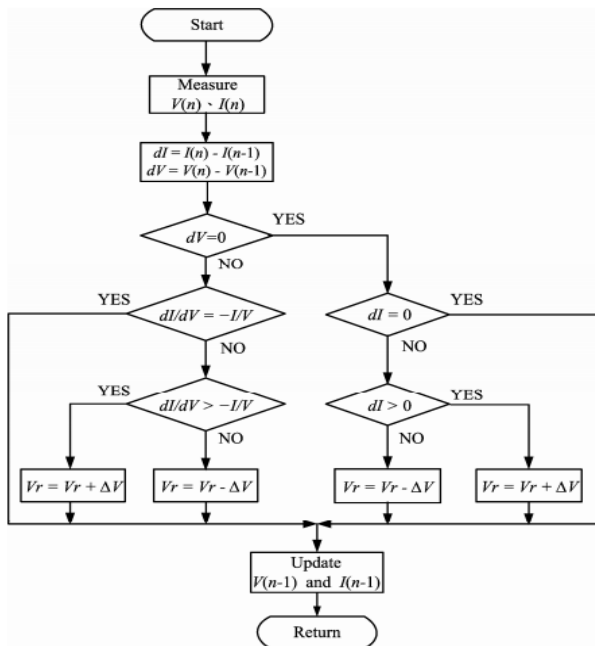


Fig.6.The flow chart of the INC method

Equations (7) and (8) are used to determine the direction of voltage perturbation when the operating point moves toward to the maximum power point. In the process of tracking, the terminal voltage of PV modules will continuously perturb until the condition of (3) comes into existence. The main difference between incremental conductance and P&O algorithms is the judgment on determining the direction of voltage perturbation. From the flow diagram shown in Fig. 6, it can be observed that the weather conditions don't change and the operating point is located on the maximum power point when  $dV = 0$  and  $dI = 0$ . If  $dV = 0$  but  $dI > 0$ , it represents that the sun irradiance increases and the voltage of the maximum power point rises. Meanwhile, the maximum power point tracker has to raise the operating voltage of PV modules in order to track the maximum power point. On the contrary, the sun irradiance decreases and the voltage of the maximum power point reduces if  $dI = 0$ . At this time the maximum

power point tracker needs to reduce the operating voltage of PV modules. Furthermore, when the voltage and current of PV modules change during a voltage perturbation and  $dI/dV > -I/V$  ( $dP/dV > 0$ ), the operating voltage of PV modules is located on the left side of the maximum power point in the P-V diagram, and has to be raised in order to track the maximum power point. If  $dI/dV < -I/V$  ( $dP/dV < 0$ ), the operating voltage of PV modules will be located on the right side of the maximum power point in the P-V diagram, and has to be reduced in order to track the maximum power point.

### 3.3.Fuzzy Logic Controller (FLC) methods

The MPPT control is based on fuzzy logic to control a switch of the multilevel inverter. Fuzzy logic controllers provide attractive features such as fast response and good performance. It is very difficult to operate the PV energy conversion systems near the maximum power point to increase the efficiency of the PV system. The current and power of the PV array depends on the array terminal operating voltage. In addition, the maximum power operating point varies with insolation level i.e., irradiance and temperature. Therefore, the tracking control of the maximum power point is a complex problem. Quick tracking under changing conditions, small output power fluctuation, simplicity and low cost are the general requirements for an MPPT. A more efficient method to solve this problem becomes crucially important. Hence, this paper proposes a method to track maximum power point using FLC. FLC is appropriate for nonlinear control. In addition, FLC does not use complex mathematics. Behaviors of FLC depend on shape of membership functions and rule base. [17]

Using seven fuzzy subsets: NB (Negative Big), NM (Negative Medium), NS (Negative Small), ZE (Zero), PS (Positive Small), PM (Positive Medium), and PB (Positive Big) the membership function values are assigned to the linguistic variables. The divider of fuzzy subsets and the shape of membership function get used to the shape up to suitable system. The value of input error  $E(k)$  and change in error  $CE(k)$  are normalized by an input scaling factor shown in Fig. 7

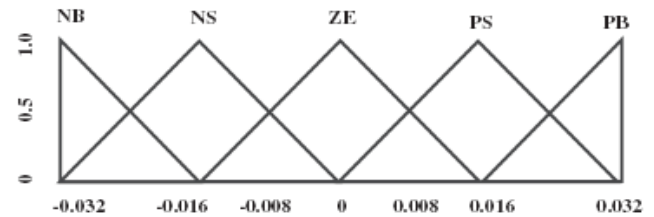


Fig.7.Fuzzy input and output membership function

In this system the input scaling factor has been designed such that input values are between -0.032 and 0.032. The triangular shape of the membership function of this arrangement presumes that for any particular input there is only one dominant fuzzy subset. The input error  $E(k)$  for the FLC can be calculated from the maximum power point as given Eq.(9) and (10)

$$(9) \quad E(k) = \frac{P_{ph(k)} - P_{ph(k-1)}}{V_{ph(k)} - V_{ph(k-1)}} \sqrt{2}$$

$$(10) \quad CE(k) = E(k) - E(k-1)$$

The output membership function of each rule is given by the minimum operator and maximum operator. Table 2 shows rule base of the FLC. The process Defuzzification is needed to compute output of the FLC, centre of gravity

method is used and the FLC output modifies the control output. Further, the output of FLC controls the switch in the inverter.

Table 2: Fuzzy rule Base

Error	Change in Error						
	NB	NM	NS	ZE	PS	PM	PB
NB	NB	NB	NB	NB	NM	NS	ZE
NM	NB	NB	NB	NM	NS	ZE	PS
NS	NB	NB	NM	NS	ZE	PS	PM
ZE	NB	NM	NS	ZE	PS	PM	PB
PS	NM	NS	ZE	PS	PM	PB	PB
PM	NS	ZE	PS	PM	PB	PB	PB
PB	ZE	PS	PM	PB	PB	PB	PB

#### 4. Multilevel inverter

The diode clamped multilevel proposed by Nabae, Takashi, and Akagi in 1981 was named as neutral point converter and was essentially a three-level diode clamped inverter. An  $m$ -level NPC inverter typically consists of  $m - 1$  capacitors on the DC bus and produces  $m$ -levels of the phase voltage. A three-phase five-level NPC inverter circuit diagram is shown in fig. 8. Each of the three phases of the inverter shares a common DC bus, which has been subdivided by four capacitors into five levels. The voltage across each capacitor is  $V_{dc}$ , and the voltage stress across each switching device is limited to  $V_{dc}$  through the clamping diodes that have been named as  $D_{1..4}$  and  $D_{1..3}$ . The key components that differ with this topology from conventional two-level inverters are clamping diodes.

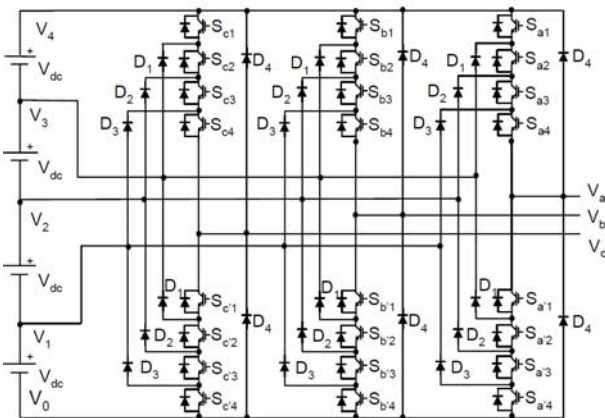


Fig.8. Circuit diagram of five- level DCMLI

Table 3: DCMLI voltage levels and switching states

Voltage $V_a$	Switch State							
	$S_{a1}$	$S_{a2}$	$S_{a3}$	$S_{a4}$	$S_{a1}$	$S_{a2}$	$S_{a3}$	$S_{a4}$
$V_4 = 4V_{dc}$	1	1	1	1	0	0	0	0
$V_3 = V_{dc}$	0	1	1	1	1	0	0	0
$V_2 = V_{dc}$	0	0	1	1	1	1	0	0
$V_1 = V_{dc}$	0	0	0	1	1	1	1	0
$V_0 = 0$	0	0	0	0	1	1	1	1

Table. 3 catalogue the output voltage levels probable for one phase of the inverter with the negative DC rail voltage  $V_c$  are always adjacent and in series. For a five-level inverter, a set of four switches is ON at any given time. [20], [21].

#### 5. Modulation Technique

A popular control method for multilevel inverters is defined as space vector PWM (SVPWM) that directly uses the control variable given by the control system and identifies each switching vector as a point in complex space

of (a, b). The SVM method uses a number of level-shifted carrier waves to compare with the reference phase voltage signals when applied to multilevel inverters. Any three-phase  $n$ -level space vector diagram consists of six sectors that all contains vector  $(n-1)^2$  combinations per sector and  $n^3$  switching. Fig.9 shows the space vector diagram five - level DCMLI, where each digit of the space vector identifier represent the voltage level to which the A, B and C phase legs are respectively switched.

The space vector waveform has been generated in the MATLAB simulink environment as shown in fig.10 and corresponding SVPWM pulse generation is shown in fig. 11, 12 and 13. The phase difference between waveforms of each consecutive phase is  $2\pi/3$  for obtaining a similar inverter output phase difference. In order to achieve better dc link utilization at high modulation indices, the sinusoidal reference signal can be injected by individual harmonics.

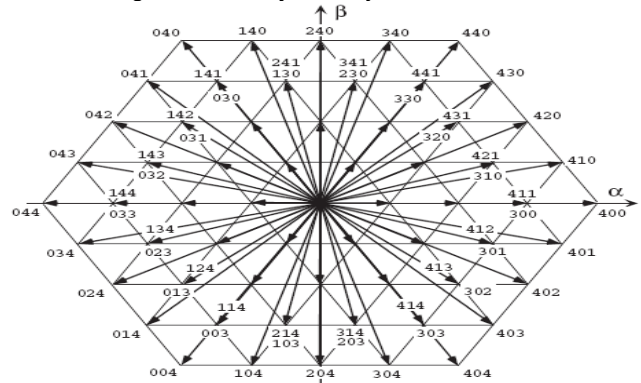


Fig.9. Space Vector States for five-Level DCMLI.

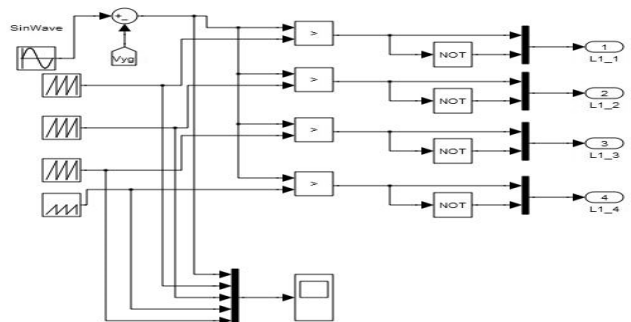


Fig.10. Matlab/Simulink diagram to generate SVPWM signals for five-level DCMLI

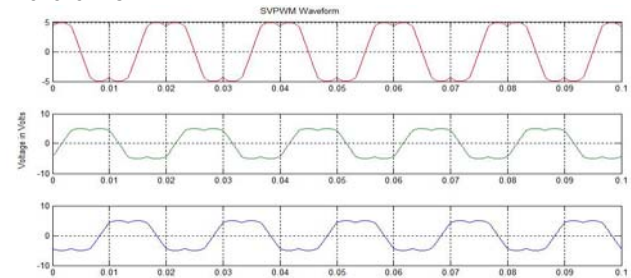


Fig.11. Space vector waveform.

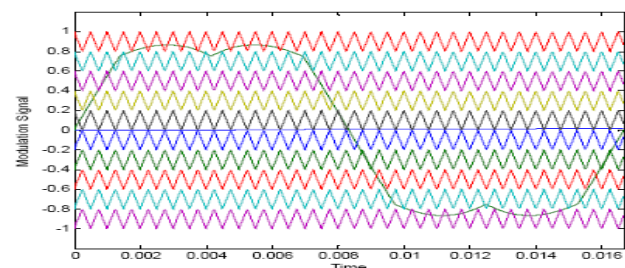


Fig.12. SVPWM signals for Five- level DCMLI

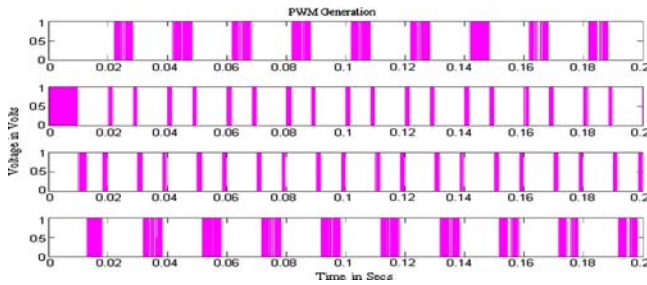


Fig.13.Five level SPWM gating pulse.

## 6. Simulations

In this paper, the insolation level (G) is changed from 700, 900 and 600 W/m<sup>2</sup> at a time period of 0s, 0.1s and 0.15s respectively. The PWM switching move toward consists of two reference signals and carrier triangular signal of 5000 Hz. The modulating index decides the shape of the output voltage of the inverter. In Fig. 14, the system response to an irradiance step is shown. The MPPT using P&O, INC and FLC tracks the working point rapidly and precisely in both conditions i.e. with and without change in irradiance level. Fig. 15. shows the results of multi DC link capacitor. It proves that the voltages are maintained constant.

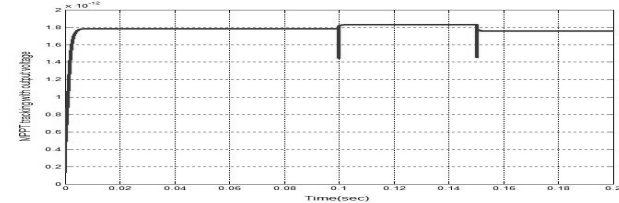


Fig.14. MPPT tracking with output voltage

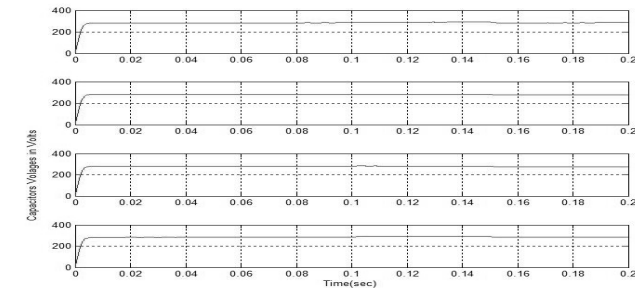


Fig.15. Five- level capacitor voltage balanced waveform

Fig. 16 illustrates the simulation result for the proposed system. The track provides good decoupling of the voltage loops  $v_d$  and  $V_q$  since the  $V_q$  remains constant under variations which shows high vigorous performances of the controllers. Thus the reactive power and active follows quietly the reference signals. The grid voltage and current are in phase thereby the power factor at the grid connection is almost unity i.e) 0.992. The performance of the FLC with the three-phase multi-level NPC also shows that output of the PV follows its reference and there are no effects for the load variation.

The THD measurement using SPWM for the proposed multi-level inverter with and without filter for the algorithms P&O, INC and FLC had shown Figs.17, 18 and 19 respectively. The THD measurement using SVPWM for the proposed multi-level inverter with and without filter for the algorithms P&O, INC and FLC had shown Figs.20, 21 and 22 respectively.

THD levels of three-phase five-level NPC with and without filters are compared in the Table IV. This proves that the proposed scheme can reduce the THD which is significant condition for grid connected PV system. The results from the table reveals that FLC mppt is best MPPT

technique in terms of THD. This proves that multilevel inverters can reduce the THD which is necessary criterion for grid-connected PV systems.

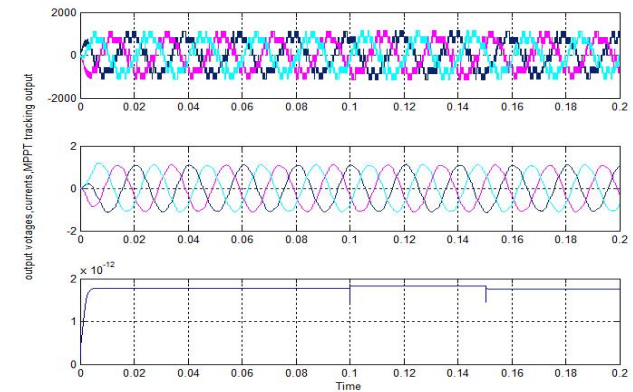


Fig.16.Five-level DCMLI output waveforms

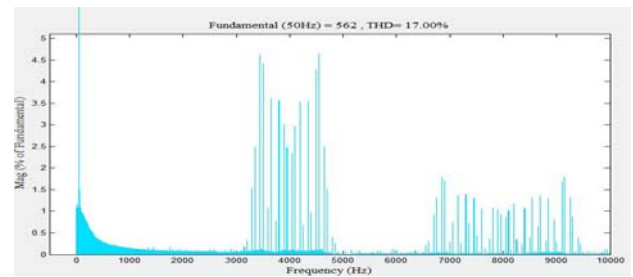


Fig.17.a THD measurement for SPWM five-level inverter without filter -P&O algorithm

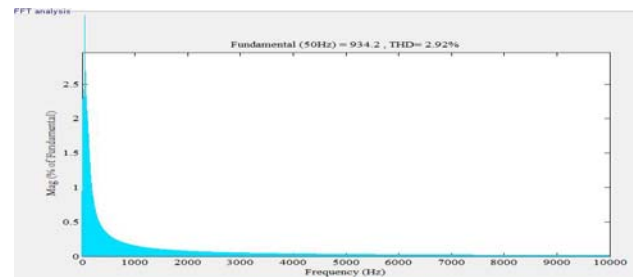


Fig.17.b THD measurement for SPWM five-level inverter with filter -P&O algorithm

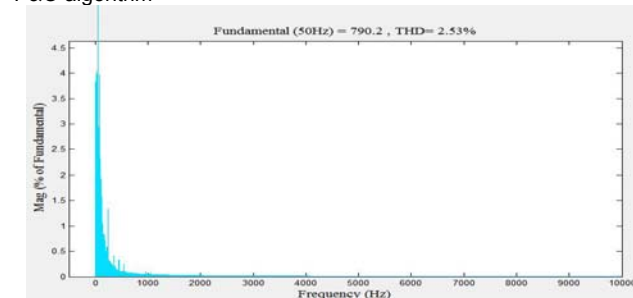


Fig.18.a. THD measurement for SPWM five-level inverter with filter -INC algorithm

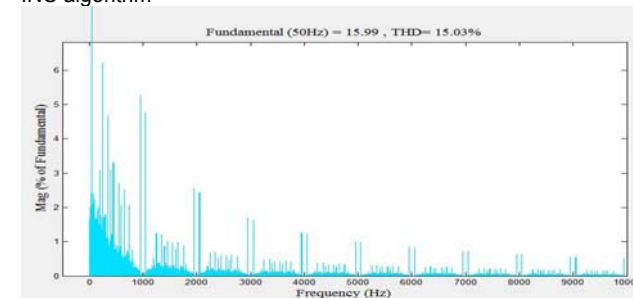


Fig.18.b. THD measurement for SPWM five-level inverter without filter -INC algorithm

Table:4 THD values for different MPPT algorithms in Percentage

Methods	With filter			Without filter		
	P&O	INC	FLC	P&O	INC	FLC
SPWM(%)	2.92	2.53	2.16	17	15.94	14.84
SVPWM(%)	2.43	2	1.33	14.21	13.01	5.2

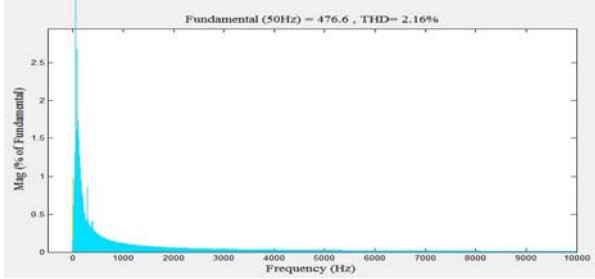


Fig.19 .a. THD measurement for SPWM five-level inverter with filter -FLC algorithm

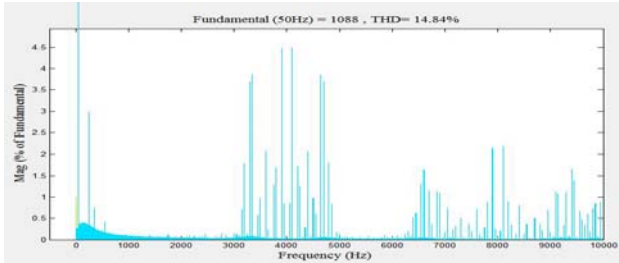


Fig.19 .b. THD measurement for SPWM five-level inverter without filter -FLC algorithm

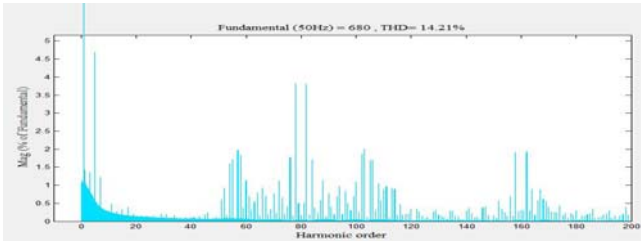


Fig.20.a THD measurement for SVPWM five-level inverter without filter -P&O algorithm

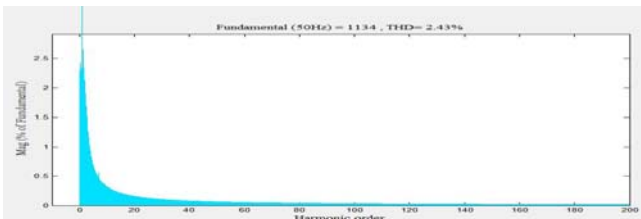


Fig.20.b. THD measurement for SVPWM five-level inverter with filter -P&O algorithm

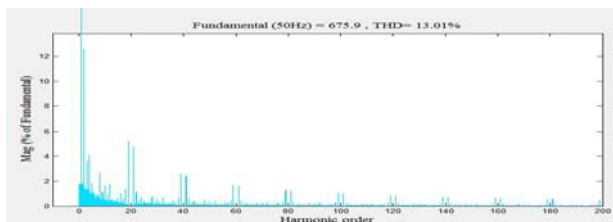


Fig.21.a. THD measurement for SVPWM five-level inverter without filter -I&C algorithm

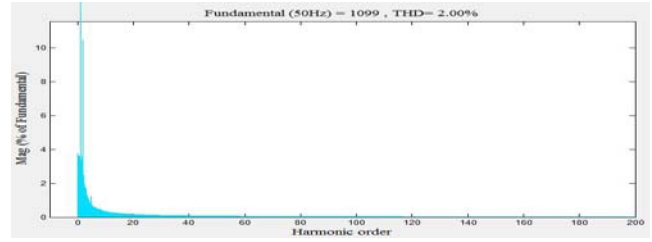


Fig.21.b. THD measurement for SVPWM five-level inverter with filter -I&C algorithm

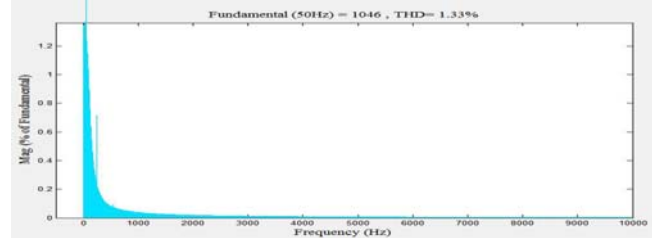


Fig.22.a. THD measurement for SVPWM five-level inverter with filter -FLC algorithm

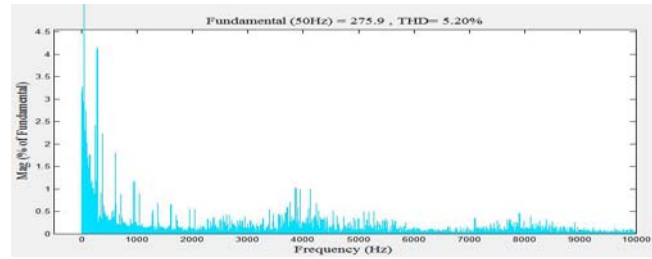


Fig.22.b. THD measurement for SVPWM five-level inverter without filter -FLC algorithm

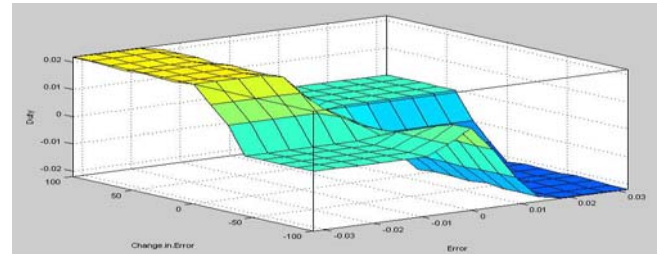


Fig.23. Optimized FLC rule surface

Fig.23. shows the Optimized FLC rule surface where the system converges to an optimal solution which is the fuzzy inference system obtained from the best swarm at the end of the simulation.

## 7. Conclusions

The purpose of this paper is to study the harmonic profile of Grid connected PV system for different MPPT methods including perturbation & observation incremental conductance and Fuzzy logic controller. The PV simulation system used in this paper is set up under Matlab/Simulink environment. The model of PV modules used in PV simulation system is established according to the electrical specifications of the PV module KC200GT . After accomplishing the model of PV modules, the models of Multi level inverter and MPPT systems are combined with it to complete the PV simulation system with the MPPT functions. The proposed fuzzy MPPT sets the optimum DC bus voltage reference for the inverter without the need for a dc-dc converter. The control of the active and reactive power is done using a PI controller. The control system

effectively tracks the maximum power and upholds the power factor close to unity under fast change in solar irradiation and temperature. The fuzzy MPPT also leads to reduced THD in the grid voltage compared with Perturb and observe and Incremental algorithm MPPT algorithm. The results are listed in Table 4

The control scheme is simulated digitally under linear and nonlinear loads and effectively tracks the maximum power. The results obtained are full of promise to use the multi level inverter in high power applications such as PV generation system with grid connected. The inverter can be easily extended by increasing the levels hence the inverter generates higher-quality output voltage and other MPPT techniques.

#### REFERENCES

- [1] Yang Chen, Keyue Ma Smedley, "A Cost-Effective Single-Stage Inverter With Maximum Power Point Tracking". *IEEE Transactions on Power Electronics*, Vol.19, NO.5, 2004, pp. 1289–1294.
- [2] K. Hussein, I. Muta, T. Hoshino, and M. Osakada, "Maximum Photovoltaic Power Tracking: An Algorithm for Rapidly Changing Atmospheric Conditions". *IEEE Proceedings. Generation, Transmission and Distribution*, 1995, 142, (1), pp. 59-64
- [3] Zagrouba, M., Sellami, A., Bouaicha, M., Ksouri, M., 2010. "Identification of PV solar cells and modules parameters using the genetic algorithms: application to maximum power extraction". *Solar Energy* 84, pp.860–866.
- [4] Santos, J.L., Antunes, F., Chehab, A., Cruz, C., "A maximum power point tracker for PV systems using a high performance boost converter". *Solar Energy* 80, 2006, pp.772–778.
- [5] Enrique, J.M., Duran, E., Sidrach-de-Cardona, M., Andujar, J.M., "Theoretical assessment of the maximum power point tracking efficiency of photovoltaic facilities with different converter topologies". *Solar Energy* 81, pp.31–38. 2007.
- [6] Hussein, K.H., Muta, I., Hoshino, T., Osakada, M., "Maximum photovoltaic power tracking: an algorithm for rapidly changing atmosphere conditions". *Proceedings of the Institution of Electrical Engineers—Generation Transmission, and Distribution* 142, pp.59–64. 1995.
- [7] A. Ravi, P.S. Manoharan, J. Vijay Anand "Modeling and simulation of three phase multilevel inverter for grid connected photovoltaic systems" *solar energy* 85, pp. 2811–2818. 2011.
- [8] F. Z. Peng, J.S. Lai, J. W. McKeever, J. VanCoevering, "A Multilevel Voltage-Source Inverter with Separate DC Sources for Static Var Generation", *IEEE Transactions on Industry Applications*, Vol 32, No.5, pp.1130-1138. September /October 1996.
- [9] M. D. Manjrekar, P. Steimer, T. A. Lipo, "Hybrid Multilevel Power Conversion System: a competitive solution for high power applications", in *Conf. Rec. IEEE/IAS Annual Meeting*, pp.1520-1527. 1999
- [10] J. Lai, F. Peng, "Multilevel Converters – A New Breed of Power Converters", *IEEE Transactions on Industry Applications*, Vol. 32, No. 3, pp. 509-517. May/June 1996.
- [11] A. Ravi, P.S. Manoharan, M. Valan Rajkumar "Harmonic Reduction of three-phase Multilevel Inverter for Grid Connected Photovoltaic System using Closed Loop Switching Control" *International review on modeling and simulation*. vol.5,N.5, October 2012. pp.1934-1942.
- [12] Tian, Y., "Analysis Simulation and DSP based Implementation of Asymmetric Three-level Single-phase Inverter in Solar Power System". Degree of Master Science, Summer Semester 2007.
- [13] Marcelo Gradella Villalva, Jonas Rafael Gazoli, and Ernesto Ruppert Filho, "Comprehensive approach to modeling and simulation of photovoltaic arrays". *IEEE Transactions on Power Electronics*. 24,(5), 2009. pp.1198 – 1208.
- [14] Fangrui Liu, Yong Kang, Yu Zhang, Shanxu Duan, "Comparison of P&O and hill climbing MPPT methods for grid-connected PV converter," *3rd IEEE Conference on Industrial Electronics and Applications*, (ICIEA 2008), 3-5 June 2008. pp.804-807
- [15] T. ESRAM, P. L. Chapman, "Comparison of Photovoltaic Array Maximum Power Point Tracking Techniques," *IEEE Transactions on Energy Conversion*, vol. 22, no. 2. 2007, pp. 439 – 449.
- [16] Hohm D.P., Ropp M.E.: "Comparative Study of Maximum Power Point Tracking Algorithms Using an Experimental, Programmable, Maximum Power Point Tracking Test Bed". *Photovoltaic Specialists Conference, 2000*. Conference Record of the Twenty-Eighth IEEE 15-22 Sept. 2000. pp.1699 – 1702.
- [17] Bouchaafa, F., Beriber, D., Boucherit, M.S., "Modeling and control of a grid connected PV generation system with MPPT fuzzy logic control". 7th International Conference on Systems, Signals & Devices, pp. 1–7. 2010.
- [18] Mouloud A. Denai, Frank Palis, Abdelhafid Zeghbeeb, "ANFIS Based Modelling and Control of Non-Linear Systems: A Tutorial", *IEEE International Conference on Systems, Man and Cybernetics*, pp. 3433 – 3438. 2004.
- [19] J. S. R. Jang, "ANFIS: Adaptive Network-Based-Fuzzy Inference System", *IEEE Transactions On Systems, Man And Cybernetics*, VOL. 23, No. 3, 1993. pp. 665 - 685
- Rodriguez, J., Lai, J.S., Peng, F.Z., "Multilevel inverters: a survey of topologies, controls, and applications". *IEEE Transactions on Industrial Electronics*. 49, (4), 2002. pp. 724–738
- [20] Kjaer, S., Pedersen, J., Blaabjerg, F., "A review of single-phase grid connected inverters for photovoltaic modules". *IEEE Transactions on Industrial Applications*. 1, (5. 2005. ), pp.1292–1306

**A. Ravi** working as Asst.Professor in Francis Xavier Engineering College Tirunelveli, India .He is currently pursuing Ph.D under Anna University, Chennai. Email: raviarmugam@gmail.com

**Dr.P.S.Manoharan** is working as Asst.Professor in Thiagarajar College of engineering, Madurai, India Email: [psmeeee@tce.edu](mailto:psmeeee@tce.edu)